MEASUREMENT OF DIELECTRIC PROPERTIES WITH SUPERCONDUCTING RESONATORS: THEORY AND PRACTICE

W. Meyer
Inst. f. Hochfrequenztechnik, Technical University
Postfach 3329, D-3300 Braunschweig, FRG

Abstract

The paper deals with theoretical and practical investigation of a test method using superconducting cavity- and helical resonators in an oscillator loop, which allows precision measurements to be performed on solid dielectrics in the range of 0.1 to 10 GHz and below 9K.The underlying formulas are an extension of the well-known perturbation formalism and are not restricted to low temperatures. Our experiments resulted in unloaded quality factors of $Q \simeq 5 \cdot 10^7$ between 0.2 and 10 GHz with a maximum Q (2.2K, 0.19 GHz) of $9 \cdot 10^8$, which enabled us to observe the smallest loss tangent so far: $\tan\delta$ (2.2K, 6.5 GHz) = $3.7 \cdot 10^{-7} \pm 5\%$ in polyethylene.

1. Introduction

In connection with recent applications of rf-superconductivity, (e.g. in generation and distribution of microwave high power /1/, superconducting high energy linear accellerators and fusion reactors /2/, or superconducting microwave communication systems /3/) there is growing need for experimental data on microwave low temperature dielectric properties of materials. This paper deals with the theoretical and practical investigation of a suitable test method, which allows high precision measurements between 0.1...10 GHz and 2...15K by using superconducting helical- and cavity resonators in an oscillator loop. We first present the underlying theory of measurement, an extension of the well-known perturbation formalism; subsequently we describe the cylindrical E_{010} - and E_{011} - cavities and helical resonators in some detail theoretically as well as their performances, and end up with some results on loss tangents of polymers which are the lowest ever measured outside the optical frequency region.

2. Theory of measurement

When a dielectric specimen is inserted into a rf-resonator, both the electric ($\vec{E}$) and magnetic ($\vec{H}$) field configurations change and quality factor Q and resonance frequency f are altered. By measuring f and Q of the unperturbed and perturbed resonator (index 1 and 2 in eqn.(1)), dielectric constant ε_2' and loss tangent $\tan\delta = \varepsilon_2''/\varepsilon_2'$ (where $\varepsilon_2 = \varepsilon_2' - j\varepsilon_2''$) can be calculated starting from the exact expression for the complex frequency shift:

$$\frac{\omega_2 - \omega_1^*}{\omega_2} = (\varepsilon_1' - \varepsilon_2' + j\varepsilon_2'') \frac{\int_{V_S} \varepsilon_0 \vec{E}_1^* \vec{E}_2 \, dV_S}{\int_{V_C} (\varepsilon_0 \vec{E}_1^* \vec{E}_2 + \mu_0 \vec{H}_1^* \vec{H}_2) \, dV_C} \qquad (1)$$

(V_C cavity volume, V_S sample volume). In eqn.(1) the unperturbed resonator is assumed to contain a lossless medium ε_1' (e.g. vacuum, or fluid helium with ε_1' (90 MHz, 4.2K)= 1.049, $\tan\delta < 10^{-10}$ /4/).
The complex frequency shift is related to measurable quantities by /5/

$$\frac{\omega_2 - \omega_1^*}{\omega_2} = \frac{f_2 - f_1}{f_2} + j \frac{1}{2} \left(\frac{1}{Q_2} - \frac{1}{Q_1} \right) \qquad (2)$$

With these equations ε_2' and $\tan\delta$ can be obtained from:

$$\frac{f_2 - f_1}{f_2} = (1 - \varepsilon_2') \frac{\int_{V_S} \varepsilon_0 \vec{E}_1^* \vec{E}_2 \, dV_S}{\int_{V_C} (\varepsilon_0 \vec{E}_1^* \vec{E}_2 + \mu_0 \vec{H}_1^* \vec{H}_2) \, dV_C} \qquad (3)$$

$$\tan\delta = \frac{1}{2} \left(\frac{\varepsilon_1'}{\varepsilon_2'} - 1 \right) \frac{f_2}{f_2 - f_1} \left(\frac{1}{Q_2} - \frac{1}{Q_1} \right) \cdot K \qquad (4)$$

Eqn.(4) with K = 1 implies the integrals from eqn.(1) to be real. This assumption is not justified in general; at least $\vec{E}_2$ consists of both real and imaginary components $\mathrm{Im}\{E_2\} \simeq \mathrm{Re}\{E_2\} \cdot \tan\delta$. Therefore K changes to values somewhat greater than 1; under the conditions: $\mathrm{Im}\{E_2\}/\mathrm{Re}\{\vec{E}_2\}$ and $(f_2 - f_1)/f_2$ smaller than 10%, which are fulfilled for little specimen dimensions and loss tangents $\tan\delta < 0.1$, the correction factor is obtained as

$$K = 2 \frac{\int_{V_S} \varepsilon_0 \vec{E}_1^* \vec{E}_2 \, dV_S}{\int_{V_C} (\varepsilon_0 \vec{E}_1^* \vec{E}_2 + \mu_0 \vec{H}_1^* \vec{H}_2) \, dV_C} \left(\varepsilon_2' - 1 + \frac{\int_{V_C} \varepsilon_0 |\vec{E}_1|^2 dV_C}{\int_{V_S} \varepsilon_0 |\vec{E}_2|^2 dV_S} \right) \qquad (5)$$

For negligible field distortions $\vec{E}_2 \simeq \vec{E}_1$ eqn.(5) is reduced to

$$K \simeq 1 - 2 \frac{f_2 - f_1}{f_2} = 2 \frac{f_1}{f_2} - 1 \qquad (6)$$

K denotes a quantitative measure for the range of application of the well-known perturbation formalism: only if $K \simeq 1$, the perturbation theory yields acceptable results.

3. Microwave resonators

We use cylindrical cavities at 7 GHz and the helical resonator of Fig.1 between 0.2 and 2 GHz. The helical resonator is a quarter-wave-shorted transmission line in which the center conductor is wound into a helix, thus having the advantage of small dimensions compared to wavelength. In contrast to cavity resonators the helical resonator has not been used before for dielectric measurements; it shows resonant frequencies approximately at odd multiples of the fundamental and covers a frequency range, which has been nearly inaccessible until now. Unfortunately the helical resonator is not suited for the exact measurement of the dielectric constant ε_2' without calibration, because field distortions at the end of the helix have to be neglected in the calculations. Furthermore, when solving Maxwell's equations for the resonator partly filled with dielectric, the helix is replaced by a fictious surface conducting only in the helix direction. Hence measured values of the frequency shift lie somewhat higher (5% in the avarage) than computational results. On that account numerical evaluations in this paper are restricted to the cavitiy resonator, but the same tendencies can be observed with the helix type.

Dielectric constant measurements: The dielectric constant is related to the resonance frequency by the characteristic equation, which is well-known for the cylindrical cavity /6/. First order approximations of Bessel functions which are valid for small deviations of the phase constant, result in a frequency shift of the E_{010}- and E_{011}- resonator when inserting a specimen ε_2':

$$\frac{f_2 - f_1}{f_1} = -\frac{\pi}{4}\frac{N_0(x_{01})}{J_1(x_{01})}\frac{x_{01}a^2}{b^2}(\varepsilon_2'-1) \simeq \simeq 1.86\left(\frac{a}{b}\right)^2(1-\varepsilon_2') \qquad (7)$$

(J_1 Bessel function, N_0 Neumann function, x_{01}=2.405, $\varepsilon_1 = 1$.
Eqn. (3) is, however, of more general interest than the characteristic equation for calculating the frequency shift, because it can be evaluated even if the transversal phase constants k_2 in the perturbed case are not known. We only have to use approximate values for k_2 (or frequency f_2) to compute the right hand side of eqn. (3) with the only condition, that k_2 must differ from k_1 in the unperturbed resonator. Otherwise, eqn. (3) delivers wrong results as demonstrated in Fig.2 where the integrals of eqn. (3) were solved analytically.
Eqn. (3) is often used in connection with the static field approximation inside the (small) specimen and the unperturbed fields outside. The analytical evaluation of eqn. (3) with $\vec{E}_2=\vec{E}_1$ leads to an equation, which is exact with respect to the E_{010} (q=0) and E_{011} -resonanance (q=1):

$$\frac{f_2-f_1}{f_1} = \frac{1-\varepsilon_2'}{2}\left\{\frac{x_{01}\left(\frac{a}{b}\right)^2}{2}\left[J_0^2(x_{01}\tfrac{a}{b}) + J_1^2(x_{01}\tfrac{a}{b})\right]\cdot \left[(q\tfrac{\pi}{h})^2 + (2-q)\left(\tfrac{x_{01}}{b}\right)^2\right] - \frac{a}{b}x_{01}J_0(x_{01}\tfrac{a}{b})\cdot (q\tfrac{\pi}{h})^2\right\} \Big/ \left\{\frac{x_{01}^2}{2}J_1^2(x_{01})\left[(q\tfrac{\pi}{h})^2 + (2-q)\left(\tfrac{x_{01}}{b}\right)^2\right]\right\} \qquad (8)$$

Figs.(3), (4) show the limited range of application of eqn.(8) which is restricted to small specimen dimensions and dielectric constants.
Eqn.(3) can also be used to determine the influence of a sample insertion hole (Fig.1) on the resonance frequency. Now $\vec{E}_1$ represents the field configuration of the ideal cavity without hole whereas $\vec{E}_2$ in addtion contains the fast decaying E_{01} -fields in the cut off waveguide. Under similar assumptions as has previously been outlined /7/, for small hole diameters 2a we end up with a frequency shift due to the sample insertion hole:

$$\frac{f-f_q}{f_q} = \varepsilon_2'\frac{a^3}{b^2h}\cdot\frac{F}{2x_{01}J_1^2(x_{01})} \qquad (9)$$

$$F = \frac{(x_{01}/b)^2}{(\frac{\pi}{h})^2 + (\frac{x_{01}}{b})^2(2-q)}$$

(For numerical results see Fig. 5). The relative error of dielectric constant measurement due to the insertion hole follows from the total differential $\delta(\varepsilon_2'-1)$ of eqn.(7); it amounts to

$$\frac{\delta(\varepsilon_2'-1)}{\varepsilon_2'-1} = -\frac{a}{x_{01}h}F\cdot\frac{f_2}{f_1}\cdot\frac{2}{\pi x_{01}N_0(x_{01})J_1(x_{01})} \qquad (10)$$

The relative error might came to several percent(Fig.6).

Dissipation measurement: According to eqn.(4) the loss tangent depends on the frequency shift as well as on the quality factor Q and field correction factor K. K appreciably deviates from 1 for the cavity resonator as is documented by Fig.7, and therefore can lead to relative errors in tanδ-measurement of more than 50% if neglected.
Another source of error is the change of the geometric factor $G=Q\cdot R_A$ (R_A=microwave resistance), when inserting the specimen. Thereby the wall currents of the resonators are modified, i.e. Q_2 in eqn.(4) is not only altered by dielectric but by ohmic loss changes, too. The equivalent change of the G-factor is displayed in Fig.8 proving this effect to be ignorable in case of high enough a Q_1 compared to Q_2. Under the same conditions the frequency dependence of $R_A(f)$ is ignorable.

4. RF-Superconductivity

Measurements of the frequency and temperature dependence of technical superconductors can be split into two contributions to the surface resistance R_A:

$$R_A(f,T) = R_{BCS}(f,T) + R_{res}(f) \qquad (11)$$

Below the critical temperature T_c the theoretical BCS-surface resistance behaves as

$$R_A \sim \frac{f^{1.7\ldots2.0}}{T}\exp\left(-\frac{\Delta}{k_B T_c}\right) \qquad (12)$$

T_c and band gap parameter Δ for relevant rf-superconductors are compiled below. The table in addition contains the improvement factor V (4.2K, 10 GHz), which relates the surface resistance of the superconductor (SC) at low temperature to Copper (Cu) at room temperature:

$$V(T,f) = R_A(Cu, 300K, f) / R_A(SC, T, f) \qquad (13)$$

	Pb	Nb	NbTi	MoRe	Nb_3Sn
T_c [K]	7.22	9.25	9.8	10.1	18.2
$\Delta\ [k_B T_c]$	2.05	1.86	1.73	1.78	2.1
V(4,2K;10GHz)	$5\cdot10^2$	$1.4\cdot10^3$	$7.5\cdot10^3$	$2\cdot10^3$	10^4

Besides R_{BCS} there appears a residual resistence R_{res} in eqn.(11), which is practically independent from temperature and is closely related to the state of the surface (smoothness, contaminations, etc.). In many cases, especially at low frequencies < 1GHz and temperatures <4.2K, the lowest surface resistance obtainable is determined by R_{res}, while even lower values could be reached in an ideal superconductor. The available data on the measured BCS-resistance is compiled in Fig.9; Fig.10 contains the values of R_{res} which were obtained with different, sometimes sophisticated surface preparation methods, as there are chemical and electrochemical polishing as well as heating processes. The straight line interpolates our own measurements for Nb, which after machining was first treated chemically in a HF/HNO_3-solution, then electron beam welded and recrystallized at 1300 C in ultra high vacuum (UHV). These resonators show unloaded Q's of typically $5\cdot10^7$ at 4.2K in the GHz region, with $9\cdot10^8$ (at 2.2K and 0.19GHz) in excess, which corresponds to an absolute accuracy of tanδ-measurement of better than 10^{-7}.

5. Experimental procedure and limitations

The needed quantites from eqn.(4): loaded quality factor, coupling factors and resonance frequency, are obtained in a test assembly which is described in detail elsewhere /8/. It consists of the transmission type resonator, which is the frequency determining element in a closed loop, in series with phase shifter, transistor amplifier or TWTA, and pin-modulator which interrupts the stationary oscillation being possible under appropriate phase conditions and sufficient amplification. Q is obtained from the exponential decay of the resonator power envelope, the coupling factors are determined by measuring the incident and transmitted powers during steady state, and the resonance frequency is measured with a microwave counter. Measurement errors do not exceed ± 2% for Q's greater than 10^4; therewith the relative error of tanδ-measurement

$$m = \sqrt{\left(\frac{1/Q_2 + 1/Q_1}{1/Q_2 - 1/Q_1}\right)^2 \left(\frac{dQ}{Q}\right)^2 + \left(\frac{\beta_1 + \beta_2}{1+\beta_1+\beta_2}\right)^2 \left(\frac{d\beta}{\beta}\right)^2} \qquad (14)$$

generally amounts to ± 5% for $\tan\delta \geq 5\cdot10^{-7}$. β_1, $\beta_2 < 10^{-2}$ are the coupling factors at the entrance and exit of the transmission type resonator, which relate the unloaded Q-factors to the measured

$$Q_{m1} = (1+\beta_1+\beta_2)^{-1} Q_1.$$

6. Experimental results

Extensive investigations on various polymers and glasses have been published elsewhere /9/,/10/ and go beyond the scope of this paper. Fig.11 as an example represents the frequency-temperature loss profile of Medium Density Polyethylene (Lupolen 4261A, BASF) with the smallest loss tangent ever measured at any frequency and temperature: tanδ (2.2K, 6.5GHz) = $3.7\cdot10^{-7}$ ± 5%. The data prove phonon-induced tunneling-relaxation of impurities or sidegroup dipoles to be the dominant loss mechanism even at temperatures far below the glass point in a frequency region, which has been fairly inaccessible for experiments until now.

7. Acknowledgements

The author wishes to thank Prof. H.-G. Unger for suggesting this work and the Deutsche Forschungsgemeinschaft for financial support.

References

/1/ W. Meyer: Superconducting microwave power generation and transmission. Microwave Power Symp. 1976, July 27-30, 1976, Leuven (Belgium)

/2/ H. Pfister: Superconducting cavities. Cryogenics 16 (1976) pp. 17-24

/3/ K. Mikoshiba et al: Superconducting coaxial cable as a communication medium with enormous capacity. IEEE Transact. COM-24 (1976) pp. 874-880

/4/ K. Mittag et al: Measurements of loss tangents of dielectric materials at low temperatures. Kernforschungszentrum Karlsruhe, IEKP-Note 121 (1973)

/5/ M. Sucher, J. Fox: Handbook of microwave measurements II, New York 1963

/6/ E. Schanda: Die Bestimmung von Dielektrizitätskonstante und Verlustwinkel im E_{010}-Mikrowellenresonator. Archiv elektr. Übertr. AEÜ20 (1966)pp. 501-505

/7/ A. Estin, Z. Bussey: Errors in dielectric measurements due to a sample insertion hole in a cavity. IRE Transactions MTT -8 (1960) pp. 650-653

/8/ W. Meyer: High sensitivity dielectric loss measurements by using superconducting microwave resonators in an oscillator loop. Electronic Letters 13 (1977) pp. 7-8

/9/ W. Meyer: Dielectric properties of polymeric materials at low temperature and high frequencies. Proceedings: 6th Internat. Cryogenic Eng. Conf., 11-14. May 1976, Grenoble, pp. 367-370

/10/ W. Meyer: Cryogenic tunneling losses at microwave frequencies in polymeric dielectrics. Solid State Commu. 22 (1977) pp. 285-8.

/11/ Proc. 5th Applied Superconductivity Conf. 1974, publ. in: IEEE Transact. MAG-11 (1975), March issue

/12/ Proc. 6th Appl. Supercond. Conf. 1976, publ. in: IEEE Transact. MAG-13 (1977), January issue

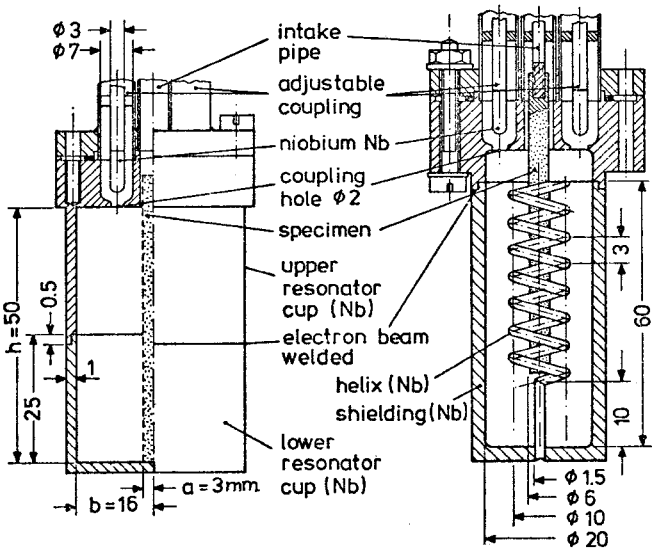

Fig.1: E_{010}-resonator (7GHz); helical resonator (200MHz).

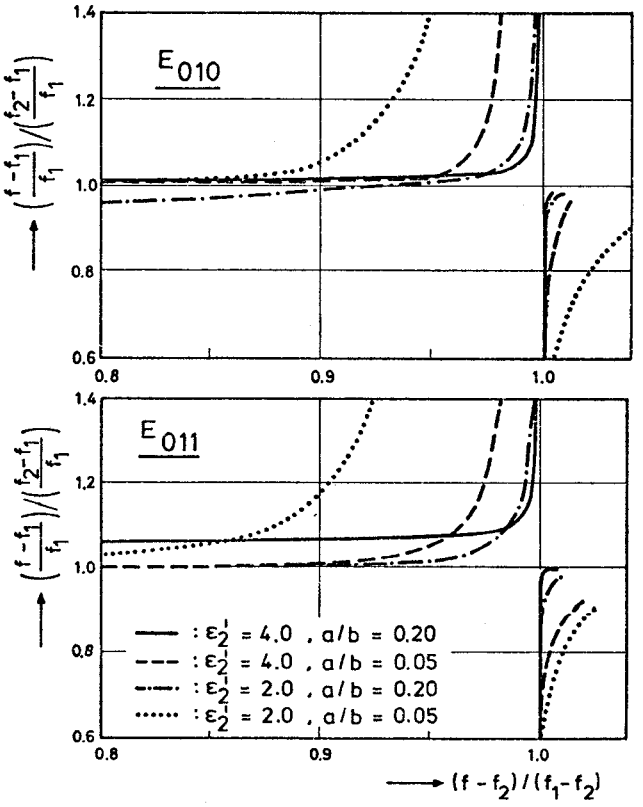

Fig.2: Solution of eqn.(3), when f is varied between $f_2<f<f_1$ in the field expressions.

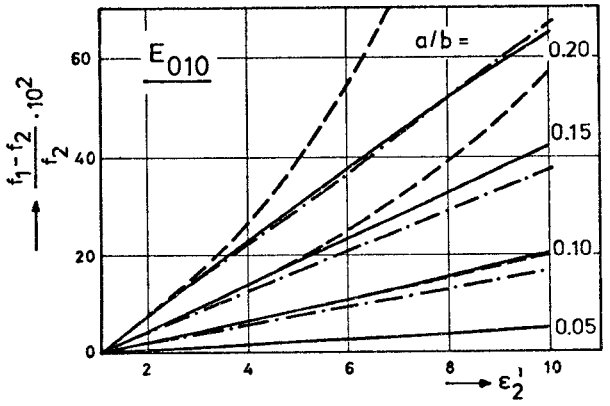

Fig.3: Frequency shift due to a dielectric ε_2' ;
exact: ——
eqn.(7): —·—·—
eqn.(8): — — —

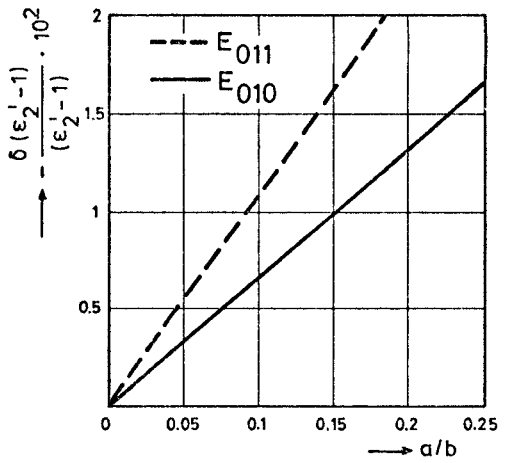

Fig.6: Relative error in ε_2'-measurement due to a sample insertion hole.

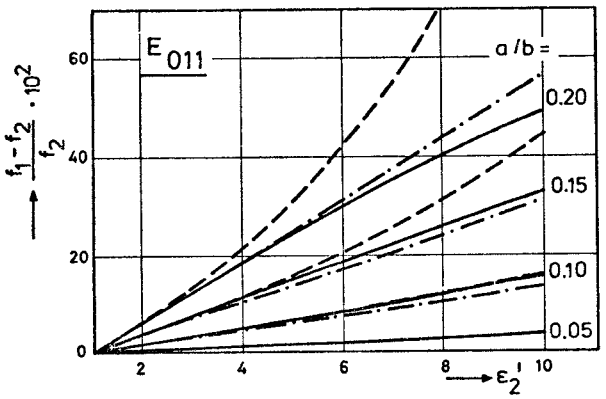

Fig.4: Frequency shift due to a dielectric ε_2' ;
exact: ——— ; eqn.(7): —·—·—·
eqn.(8): — — — —

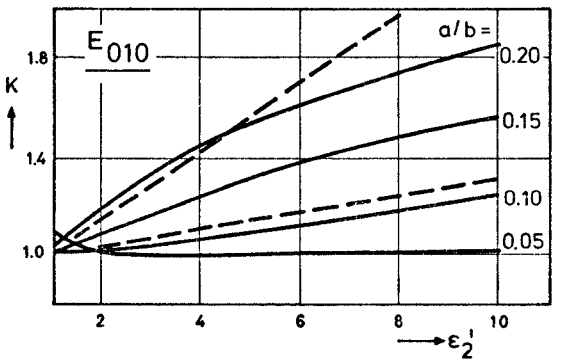

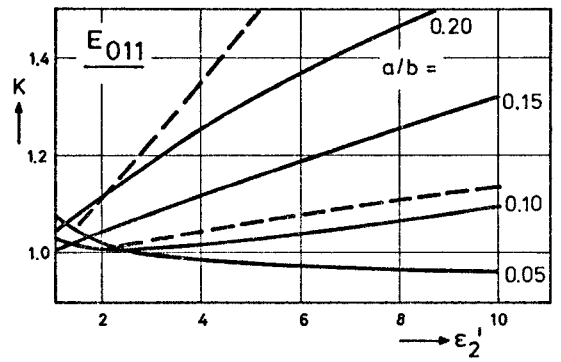

Fig.7: Correction factor K of cavity resonator;
exact expression eqn.(5) : ———
approximation eqn.(6) : — — —

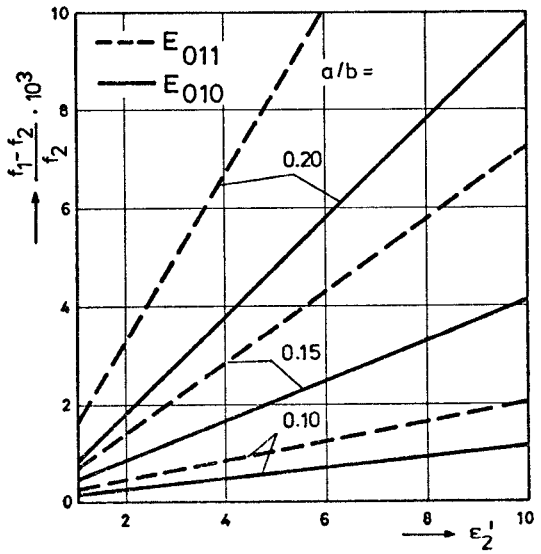

Fig.5: Change of resonace frequency f_2 due to a sample insertion hole.

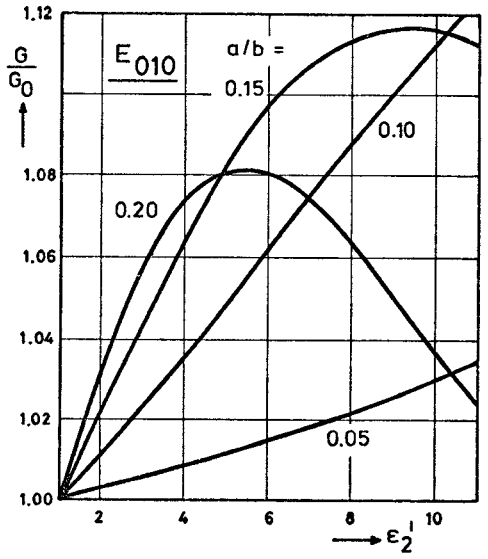

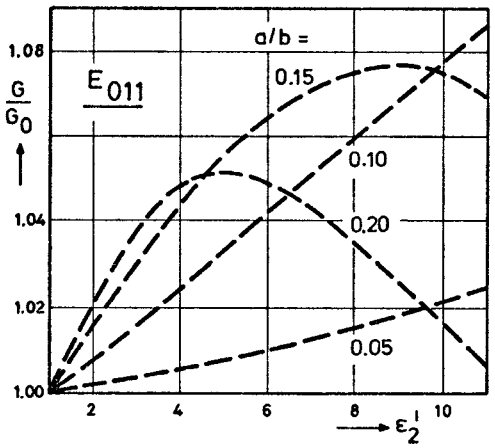

Fig.8: Change of geometric factor G; $G_0 = 300\Omega$ (empty cavity).

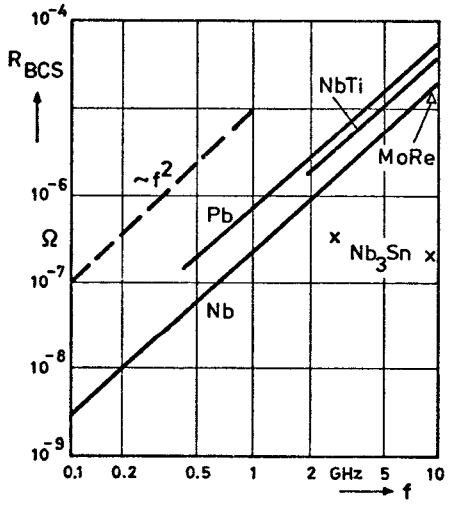

Fig.9: BCS-Surface resistance R_{BCS}; experimental data, partly taken from /11/,/12/.

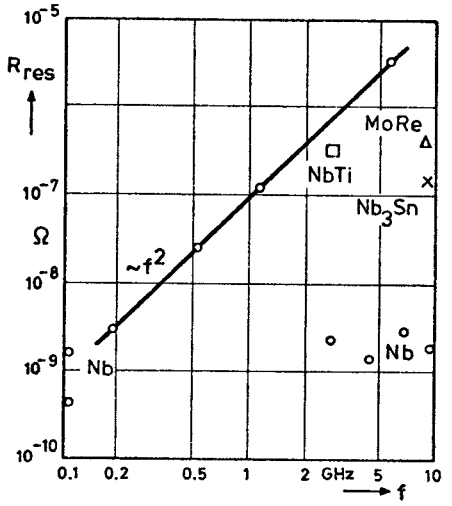

Fig.10: Residual surface resistance R_{res}; experimental data, partly taken from /11/,/12/.

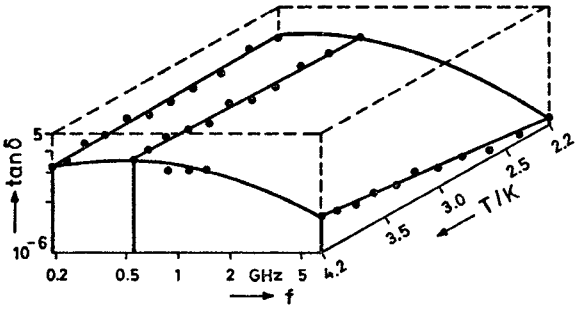

Fig.11a: Frequency-temperature loss profile of polytetrafluoroethylene.

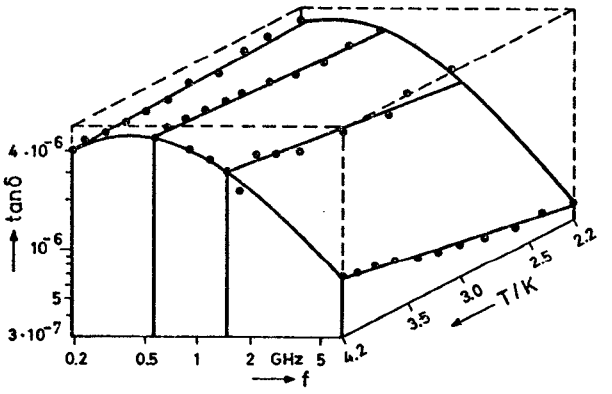

Fig.11b: Frequency-temperature loss profile of polyethylene.